PROCEEDINGS OF SCIENCE

When particle physics meets the dark Universe

Nicolao Fornengo*
Department of Physics, University of Torino and Istituto Nazionale di Fisica Nucleare (INFN), via P. Giuria 1, I-10125 Torino, Italy
E-mail: nicolao.fornengo@unito.it , fornengo@to.infn.it

Among the indirect–detection signals of dark-matter particles present in our Galaxy and in the extragalactic environment, radio signals have recently gained interest since it has been shown that current and proposed radio detectors could have the capabilities to identify a signal over the astrophysical radio background, at the same level if not better than the other techniques based on higher–energy multiwavelength emission or low–energy cosmic rays. In this report we summarize the field of dark matter searches in the radio band, by discussing both the galactic signal and the cosmological emission. A recently reported extragalactic excess in the radio sky, commonly referred to as the "ARCADE excess", will be discussed and shown to be compatible with a dark matter emisison.

VIII International Workshop on the Dark Side of the Universe,
June 10-15, 2012
Rio de Janeiro, Brazil

*Speaker.

PoS(DSU 2012)003

1. Introduction

The nature of non–baryonic Dark Matter (DM) is one of the great puzzles of modern Cosmology. A non–gravitational detection of DM would be a fundamental step toward the understanding of its properties. This could be obtained in several ways, the most promising and popular methods being direct searches in low–background underground experiments and indirect detection methods. Particle searches at colliders can offer a complementary tool to identify the fundamental properties of DM.

Indirect detection techniques are based on the identification of the products of DM annihilations or decays, notably neutrinos, antimatter and photons. Indirect searches are particularly promising if DM is in the form of Weakly Interacting Massive Particles (WIMPs). In the early Universe, WIMPs decouple non–relativistically from the thermal plasma and inherit the correct relic abundance if they possess a thermally averaged annihilation cross section of the order of $\langle \sigma v \rangle = 3 \times 10^{-26}$ cm^{3}s^{-1}. Annihilations of WIMPs inside galaxies are able to inject large amounts of relativistic electrons and positrons, which then produce synchrotron radiation by interacting with the galactic magnetic fields . This is a generic prediction of WIMP models, except for the peculiar case of WIMP candidates annihilating only into neutrinos. For galactic magnetic fields with a strength of the order of μG and electrons energies below about 10 GeV, synchrotron emission occurs at frequencies around and below the GHz, *i.e.* in the radio band. Radio observations appears therefore to be appropriate tools for indirect WIMP searches and they have been extensively discussed in the context of WIMP annihilations in our Galaxy or in the extragalctic environment [1, 2, 3, 4, 5, 6, 7, 8, 9, 10, 11, 12, 13, 14, 15].

In this note we will discuss the relevance of radio signals for WIMP dark matter detection. We will focus on both the galactic and extragalactic components, considering also the possibility to extract information from the angular correlations on the radio sky, profiting of the good angular resolution of radio detectors. Notably, we will comment on a detected extragalactic radio excess below few GHz, commonly called the "ARCADE excess", and we will show that this potential excess is compatible with a signal from DM annihilation [1]. Future and foreseen radio detectors will be able to test this hypothesis. These note is based on Refs. [1, 2, 3], where additional details can be found.

2. The galactic emission

Dark matter annihilations in the Galactic halo inject relativistic electrons and positrons which then generate a synchrotron radiation when they interact with the galactic magnetic field. As shown in Ref. [2], the low–frequency range (from 22 to 1420 MHz) offers a new window in the search for DM, especially for those low–mass WIMPs which are currently under deep scrutiny in direct detection searches [16, 17, 18]. Indeed, for magnetic fields of μG, as is typical in the Galaxy, synchrotron emission below GHz–frequency is produced by electrons and positrons with energies well below 10 GeV. In particular, WIMP candidates annihilating into light leptons with a "thermal" annihilation cross-sections can be strongly constrained for masses $M_{\rm DM} < 10\,{\rm GeV}$ [2].

Details of the calculation of the galactic radio emission are found in Ref. [2], where five different radio surveys with frequencies below few GHz and a large sky coverage were selected

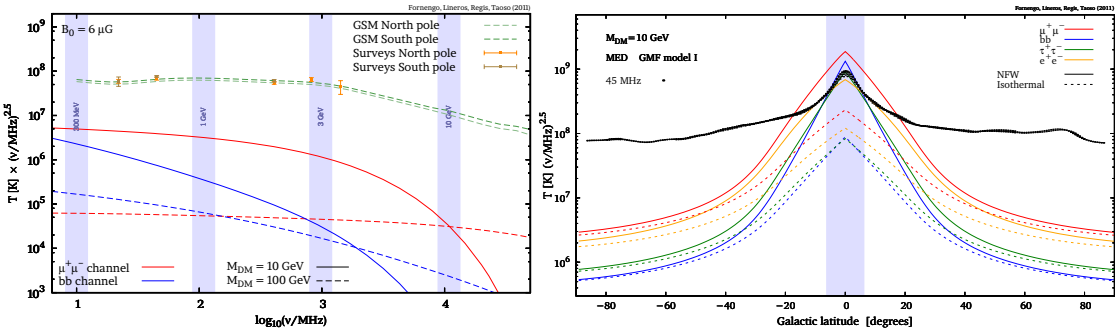

Figure 1: Left panel: Temperature versus frequency calculated at the galactic poles ($b = \pm 90^\circ$) for $\mu^+\mu^-$ and $b\bar{b}$ annihilation channels, $M_{\rm DM} = 10, 100$ GeV. We adopt a galactic magnetic field as in Ref. [2], an NFW dark matter profile and the median propagation model for electrons/positrons in the Galaxy [2]. The data points denote the temperatures at the north and south galactic poles, averaged over a 10° circle. Right panel: Temperature versus galactic latitude at 45 MHz. Data refer to a thin strip $|l| < 3^\circ$, with l the galactic longitude. Lines are predictions for DM models for $l = 0^\circ$. The vertical blue band corresponds to $|b| < 10^\circ$ directed towards the Galactic center. Predictions are showed for different annihilation channels, NFW and isothermal DM profiles, for the same galactic magnetic field and propagation parameters as in the left panel. Figures adapted from Ref. [2].

as the most suitable for DM analyses. As a first result, which shows the capabilities of radio measurements for DM studies, we report in the left panel of Fig. 1 the average temperature observed at the galactic poles at different frequencies. The data have been averaged over a 10° circle. The vertical bands identify the average frequency of the synchrotron radiation produced by electrons of a given energy and suggest that synchrotron emission produced by < 100 GeV DM particles peaks at sub–GHz frequencies. These frequencies are therefore particularly suitable to search for light or intermediate DM masses. Moreover, both WIMP models with dominant hadronic annihilation final states and leptophilic light–WIMP models, induce a synchrotron spectrum which is softer than the observed galactic one. One of the main motivations of this study therefore resides in the fact that low radio frequencies have the largest constraining power for such WIMP models.

The right panel of Fig. 1 compares observations and DM emissions at 45 MHz for different DM models and astrophysical configurations. The data refer to a thin strip crossing the galactic center and perpendicular to the galactic plane ($|l| < 3^\circ$). The figure shows that it is viable to search for a DM signal outside the inner galactic center region ($|b| > 10^\circ$). Inside this region, displayed by the blue band, the astrophysical uncertainties on the propagation model, the DM distribution, and the contamination from the astrophysical background become more important [2]. As expected, for a cored isothermal model for the galactic DM halo, the emission is strongly reduced at small galactic latitudes and longitudes, as compared to the emission from a more pronounced NFW profile. The scaling of the signal with the magnetic field strength is $\propto B^{-2}$. In general, the emission does not significantly change for different typical assumptions galactic magnetic field spatial profiles, unless one considers a large mismatch between the size of the diffusion box and the scale at which the magnetic field becomes suppressed [2].

While the observed radio emission is dominated by the astrophysical background, Fig. 1 nevertheless suggests that DM could substantially contribute to the radio flux, especially close to the

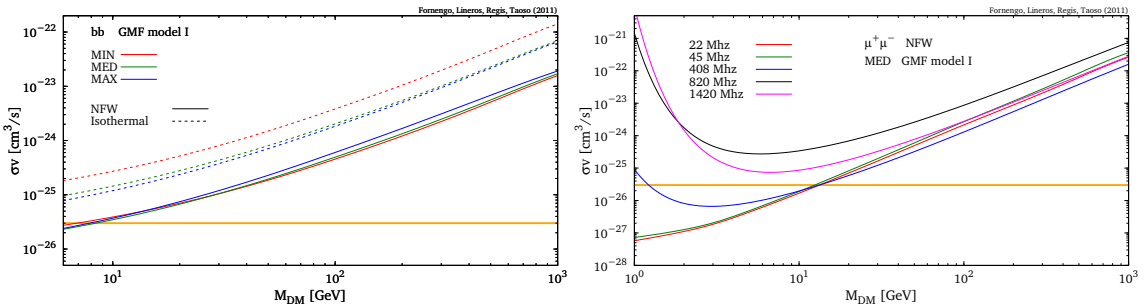

Figure 2: Left panel: upper bounds on the DM annihilation cross section (σv) versus the DM mass, for annihilation into $\bar{b}b$ quarks, for the NFW and isothermal DM profiles and for a galactic magnetic field as in Ref. [2]. The horizontal line shows the value of the "thermal" annihilation cross section. The bounds are from all sky and from a combination of 5 frequency skymaps, as in Ref. [2]. Right panel: upper bounds on the DM annihilation cross section (σv) versus the DM mass, for annihilation into the $\mu^+\mu^-$ channel, for the NFW and for a galactic magnetic field as in Ref. [2]. The plot shows the dependence of the bound on individual frequencies. The horizontal line shows the value of the "thermal" annihilation cross section. Figures adapted from Ref. [2].

galactic center or just away from it. Certainly a DM detection is challenged by the large uncertainties which affect the determination of the background. In the following, in order to be conservative we directly use the present observational data to constrain DM models, without attempting any background subtraction [2]. This will prove to be already quite constraining, especially for light leptophilic WIMPs.

The bounds on the dark matter parameter space are therefore conservatively inferred requiring that dark matter synchrotron emission does not exceed the data, without attempting any subtraction of an astrophysical component (background). Our procedure is the following: the sky is subdivided in 232 patches obtained as explained in Ref.[2]; we then compute the average DM radio emission ($T_{\rm DM}$) and the average observed radio flux ($T_{\rm obs}$) in each patch covered by the data in the data samples we use (notice that most of the surveys do not cover all the sky [2]). The constraints inferred from each patch is obtained requiring that: $T_{\rm DM} \leq T_{\rm obs} + 3\sigma$ where σ is the rms temperature noise [2]. This calculation is repeated for all the frequencies and then a bound on the DM annihilation cross section (σv) is set by taking the most constraining patch. Some of the results are summarized in Fig. 2. The bounds do not dramatically vary for different annihilation channels. We find that models with DM masses $M_{\rm DM} < 10$ GeV and "thermal" value of the annihilation cross section $(\sigma v) = 3 \times 10^{-26}$ cm^3 s^{-1} are strongly constrained in the case of the NFW profile (especially for a leptophylic WIMP), while the bounds drastically weaken for an isothermal DM profile, since it possesses a much lower DM density in a large region around the Galactic center. For an NFW DM profile and for the $\mu^+\mu^-$ and e^+e^- annihilation channels, thermal values of (σv) can be already excluded for $M_{\rm DM} < 4-6$ GeV [2]. Dependencies on the electron/positron propagation models and on the galactic magnetic field properties, and how these uncertainties reflect on the determination of the bounds on the DM properties, are discussed in details in Ref. [2].

The relevance of the different radio surveys (which cover different frequency ranges) in determining the constraints on the DM properties are shown in the right panel of Fig. 2. As anticipated above, the lowest frequencies are more constraining for low DM masses ($M_{\rm DM} < 10$ GeV) while

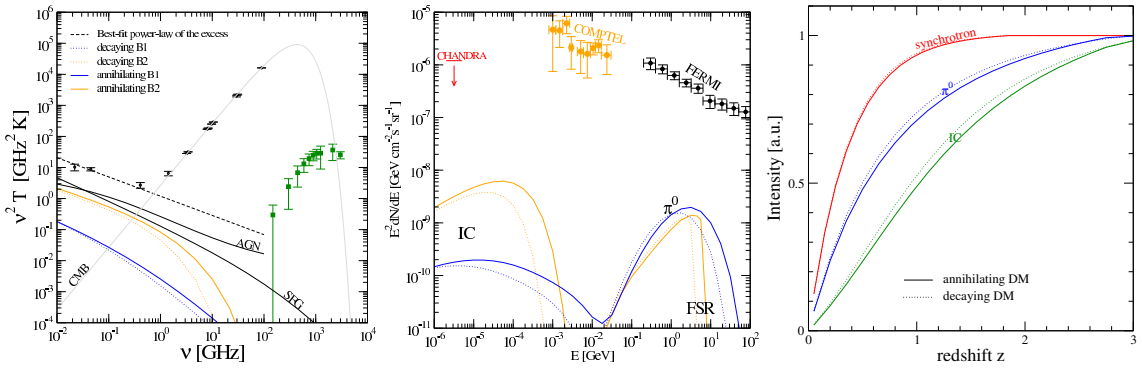

Figure 3: Extragalactic radio (left panel) and X/gamma ray (central panel) emissions for different DM benchmark in the annihilating (solid) and decaying (dotted) cases (B1: WIMP with a 100 GeV mass, producing b quarks; B2: WIMP with a 10 GeV mass, producing muons; in both cases, the annihilating WIMP has a "thermal" cross section (see Ref. [3] for additional details). For the radio case, main astrophysical source contributions (black–solid), CMB (black–dotted), and the best–fit of ARCADE data (black–dashed) are shown [19]. The right panel shows contributions at different redshifts of the emissions produced by synchrotron radiation at 1 GHz, inverse Compton scattering on CMB at 1 MeV, and π^0-decay at 1 GeV, in the benchmark case B1 (all normalized to unity). Figures adapted from Ref. [3].

$\mathcal{O}$(GHz) frequencies become relevant for heavier DM candidates. Let us also remark that the constraining power of a single survey also depends on the fraction of sky coverage and on its sensitivity: this is visible in the right panel of Fig. 2, where the 820 MHz survey provides worse constraints than the 1420 MHz one.

3. The extragalactic emission

Dark matter annihilation (or decay) in cosmic structures external to our Galaxy may produce a radio flux of extragalactic (or cosmological origin). A detailed analysis on this topic has been performed in Ref. [3], to which we refer for all the details. Ref. [3] showed that three relevant observables may be fruitfully used to study the cosmological radio emission: flux intensity, differential number counts of extragalactic sources and angular correlations of the radio sky–temperature. Ref. [3] showed that source counts and angular correlation data could be particularly relevant to disentangle the DM contribution from astrophysical sources, such as radio loud active galactic nuclei (AGN) and star forming galaxies (SFG). It was also noticed that cosmological radio emission induced by WIMP DM has a fast decrease with redshift [3]: the main contribution arises from structures at $z \ll 1$. Moreover, DM halos can significantly contribute to the source counts at brightness below the μJy level. Therefore, a specific property of the extragalactic WIMP–induced source population is to peak at low redshift and low brightness. This hypothesis can be tested by radio telescopes with flux sensitivity able to reach the μJy level, that will be reached by upcoming radio experiments, in particular by the Square Kilometer Array (SKA).

A feeling about the expected DM signals and how they compare to astrophysical emissions can be obtained by analyzing a few relevant benchmark models. Let's consider a WIMP DM candidate (model B1) with mass $M_{\rm DM} = 100$ GeV, "thermal" annihilation cross section $\langle\sigma_a v\rangle = 3 \cdot 10^{-26}\,{\rm cm}^3{\rm s}^{-1}$ and final state of annihilation into quarks $b\bar{b}$ (and similarly a decaying case with

lifetime $\tau = 4 \cdot 10^{28}$ s). Motivated by recent indications from direct detection experiments (DAMA [16], CoGeNT [17], and CRESST [18]) and by a possible DM interpretation of the ARCADE excess [1] (discussed in the next Section), we introduce also a DM candidate (model B2) with mass $M_{\rm DM} = 10$ GeV, again with "thermal" annihilation rate, but annihilating into a purely leptonic final state $\mu^+ - \mu^-$ (to enhance the synchrotron signal), together with a decaying case with $\tau = 5 \cdot 10^{27}$ s. A detailed discussion on the DM halo mass function, the halo concentration, the DM distribution in halos and the cosmological model adopted in this analysis are discussed in Ref. [3]. No substructures are considered in this benchmark scenario and the minimum halo mass is set to $M_{\rm cut} = 10^5 M_\odot$. The magnetic field is assumed to be constant in space and time with $B = 10\,\mu G$, and e^+/e^- are assumed to radiate at the same place where they are injected. The validity of these assumptions and the impact of relaxing them is analyzed in Ref. [3].

The left and central panels of Fig. 3 show total intensities: in the radio band (left panel) and in the X and gamma bands (central panel). X and gamma emission are expected to be counterpart of DM radio emission, since the same electrons produced by DM annihilation or decay and that produce a radio signal as synchrotron radiation, can induce higher energy photons by inverse Compton (IC) scattering on the CMB and radiation fields. Moreover, if the DM particle produces hadronic final states in its annihilation/decay process, these states necessarily produce gamma–rays, the most prominent channel being π^0 decays. In the case of annihilation/decay into leptons, final state radiation again contributes to the X and gamma bands. Note that the DM contribution in those benchmark scenarios is roughly at the same level of the astrophysical emissions and that the extra–galactic sky temperature reported by the ARCADE 2 collaboration [31] cannot be explained by ordinary models of AGN plus SFG. In Ref. [1] we discussed the possibility of interpreting the ARCADE data in terms of a DM–induced synchrotron emission. WIMP models can actually account for the excess, with viable scenarios being only slightly more optimistic than the benchmark cases considered here [1]. This possibility of interpreting the so–called "ARCADE excess" in terms of a DM signal is further discussed in the next Section. Comparing the left and central panels of Fig. 3, one can see that radio extragalactic data are more constraining than the gamma–ray counterpart for WIMP models with a dominant leptonic annihilation/decay channel (approximately by one order of magnitude in the B2 case); on the contrary, for WIMP models with significant π^0 production (as the B1 benchmark), gamma and radio data have roughly the same constraining power.

In Fig. 3 we have considered energy losses due to synchrotron radiation and to IC scattering on CMB only. The effect of the electron and positron interactions with interstellar radiation fields (ISRF) is difficult to model since it is mostly related to the properties of the astrophysical sources hosted within each halo, rather than to the halo mass. However, the IC loss associated to the ISRF is expected to be subdominant in the extragalactic signals. To corroborate this point, we performed a calculation with energy losses on a simple ISRF with constant density of $1\,{\rm ev\,cm^{-3}}$ in all halos at any mass M and redshift z. This density is of the order of the mean optical ISRF density of the Milky Way and can be considered as an overestimate of the actual field, since it is known that either lager (*e.g.* cluster) and smaller (*e.g.* dwarf spheroidal galaxies) structures have much lower density. The effect on the total intensity curves shown in Fig. 3 reflects in an overall depletion of about 15% [3]. We can therefore assume energy losses due to IC on ISRF as a (relatively) subdominant effect.

In the right panel of Fig. 3 we show the redshift distribution of main radio, X–, and gamma–ray signals. Inverse Compton scattering on CMB is completely set by the evolution of the DM

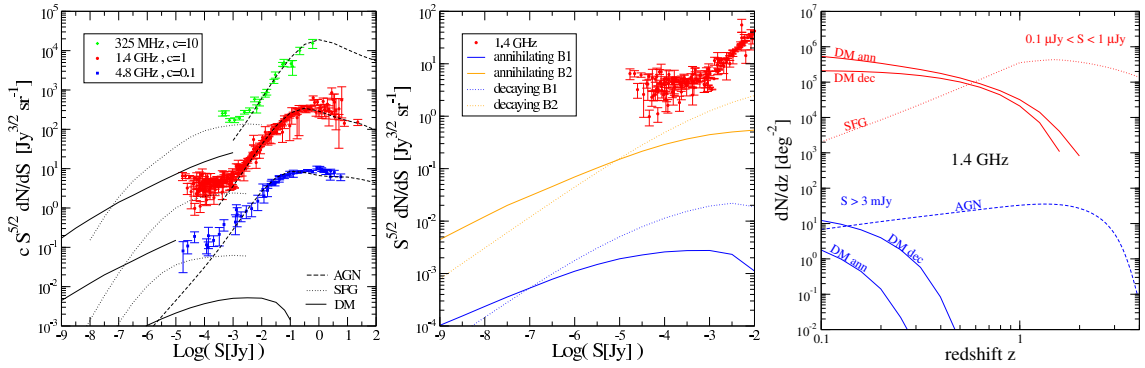

Figure 4: Left panel: differential number counts for active galactic nuclei (dashed), star–forming galaxies (dotted), and the benchmark B2 annihilating DM model (solid) described in Fig. 3. Data are taken from Ref. [20]. Data and curves referring to different frequencies are multiplied by a factor c (given in the figure inset) for clarity. Central panel: differential number counts at 1.4 GHz for the benchmark DM models described in Fig. 3. Right panel: redshift distribution of bright ($S > 3$ mJy, lower) and faint ($0.1\,\mu\text{Jy} < S < 1\,\mu\text{Jy}$, upper) astrophysical sources (only the dominant population is shown) and the benchmark DM models B2. Figures adapted from Ref. [3].

spatial distribution. Indeed, the dilution of CMB energy density due to the expansion of the Universe affects both energy losses and IC power, producing basically no net effect on the emission. There can be a further suppression in the emission at low z if synchrotron losses take over at late times. Moreover, the location of the IC peak is approximately redshift–independent (and therefore the same occurs for the energy of the emitted electrons), since the factor $1/(1+z)$ arising from emission to the observer is exactly compensated by the increase $(1+z)$ in the CMB photon energy [21]. For π^0-decay emission, there is an additional decrease with redshift which depends on the WIMP annihilation/decay energy spectrum, since the emission is given by $dN_\gamma/dE[(1+z)E]$. Correspondingly, the contribution at high redshifts becomes less prominent as compared to the IC on CMB case. An important conclusion that can be obtained from the right panel of Fig. 3 is that the synchrotron total intensity is given by emissions at low redshift, lower than in the case of the IC case. This is easily understood as due to the rapid increase in the energy loss associated to IC scattering on CMB (that scales as $(1+z)^4$), while a large increase with z of the magnetic field is not expected.

Let's move now to the discussion of number counts, shown in Fig. 4. The annihilating WIMP model B2, which leads to a total intensity comparable to astrophysical contributions (as shown in Fig. 3), is now compared to AGN and SFG counts in the left panel of Fig. 4. AGN contributions largely dominate at strong brightness, while SFGs emerge below mJy–fluxes. The DM emission becomes dominant in the sub-μJy regime. The corresponding decaying case has a steeper spectrum (see the central panel of Fig. 4): therefore, although at large brightness it is relatively more important than the annihilating case (but still subdominant), it starts dominating only much below the μJy level. This occurs because of the ρ^2 scaling in the annihilating case (combined with the increase of the concentration parameter as the halo mass decreases) which makes the smaller and fainter structures relatively more important than larger and brighter halos.

The right panel of Fig. 4 shows again (along the same line of the right panel of Fig. 3) that

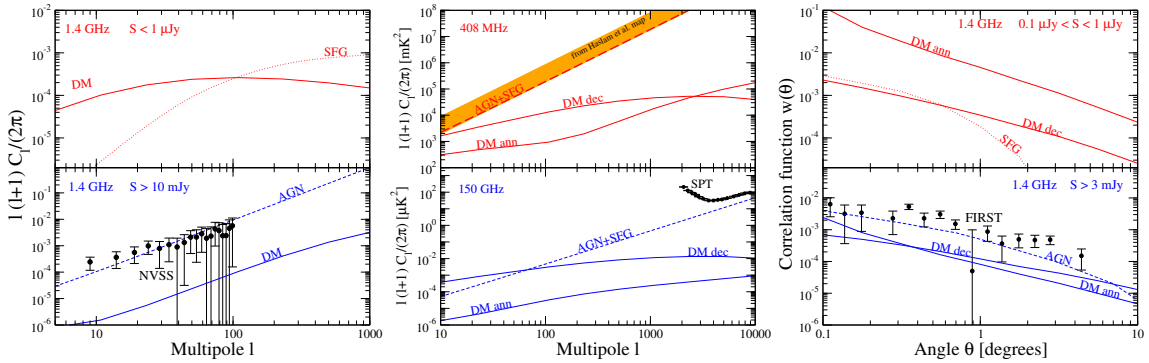

Figure 5: Left panel: angular power spectrum at 1.4 GHz of bright ($S > 10$ mJy, lower) and faint ($S < 1\,\mu$Jy, upper) astrophysical sources (only the dominant population is shown) and the DM benchmark B2 for the annihilating case, described in Fig. 3. Data points are derived from NVSS as in Ref. [22]. Central panel: angular power spectrum including contributions from sources at all brightness at 408 MHz (upper: observational band derived from Ref. [23], see Refs. [24, 25]) and 150 GHz (lower: data from Ref. [26]) for astrophysical sources, benchmark DM models B2 (at 408 MHz), and a WIMP model (at 150 GHz) with $M_{\rm DM} = 1$ TeV and $\langle\sigma_a v\rangle = 3 \cdot 10^{-23}\,{\rm cm}^3{\rm s}^{-1}$ (annihilating) or $\tau = 10^{26}$ s (decaying) (*i.e.* fitting the PAMELA positron excess [27]). Angular correlation function at 1.4 GHz of bright ($S > 3$ mJy, lower) and faint ($0.1\,\mu{\rm Jy} < S < 1\,\mu{\rm Jy}$, upper) astrophysical sources (only the dominant population is shown) and DM benchmark models B2 (data are from [28]). Figures adapted from Ref. [3].

most of the WIMP–induced radio emission comes from sources at very low redshift. For large brightness, AGN dominates and the DM emission is subdominant almost at all redshift. On the contrary, in the sub-μJy regime, DM sources are more numerous than SFG up to $z \sim 1$. The exact shape of SFG counts is not completely understood yet, and curves in Fig. 4 represent one possible model. However, the overall normalization and the fact that the SFG contribution peaks at $z > 1$ are rather robust predictions [20]. This means that we can firmly conclude that a WIMP source population which provides a significant contribution to the total intensity has to dominate in the source count at low brightness ($S < \mu$Jy) and low redshift ($z < 1$).

As a last observable for the cosmological radio emission, we consider the angular correlation of radio sources, reported in Fig. 5. The dimensionless angular power spectrum C_ℓ and the angular correlation function w are normalized to the mean intensity $\langle I\rangle$ and to the number counts N corresponding to the astrophysical contributions, respectively. Regarding the power spectrum, the one–halo term, which basically behaves as a Poisson–noise term ($C_\ell \sim$ const) up to very large multipoles, dominates at large brightness (namely, at brightness currently covered by data), where the DM contribution is then much smaller than the AGN one. In the sub–μJy regime, the two–halo term is instead the most important one, and the DM population starts dominating, especially at low multipoles, *i.e.* large scales. Notice also that the DM power spectrum is quite different from a flat C_ℓ (except when considering only the brightest halos): this tells us that it is mostly given by the two–halo term. This again occurs because the DM source peaks at very low redshift, which explains also why the DM tends to have more power on large scales. For data corresponding to observations which integrate over all brightness, like the Haslam *et al.* map [23] at 408 MHz and the SPT survey [26] at 150 GHz, the C_ℓ are mostly due to the brightest objects and the DM contribution gives only a marginal contribution at $\ell < 100$ (where, however, any estimate of the extragalactic

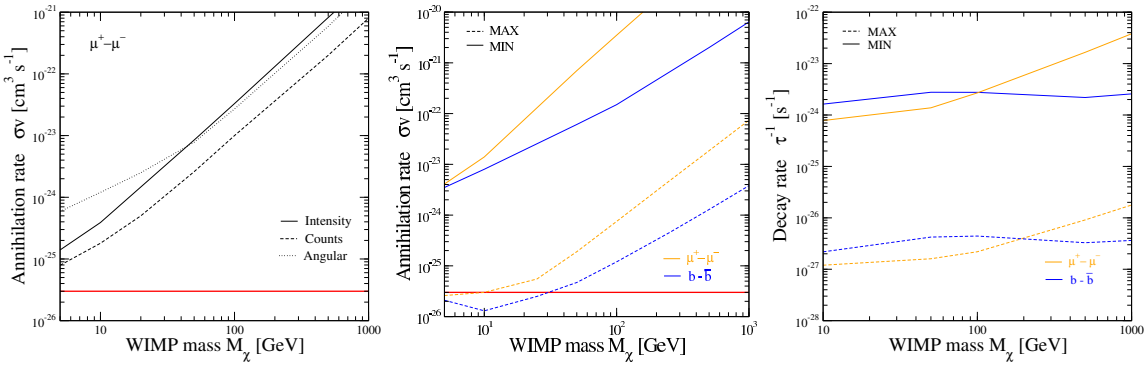

Figure 6: Left panel: bounds obtained from total intensity (solid), source counts (dashed), and angular correlation (dotted) for WIMPs with dominant annihilation channel $\mu^+\mu^-$. Clustering and other astrophysical assumptions are as described in Ref. [3]. The reference "thermal" annihilation value $\langle\sigma_a v\rangle = 3\cdot 10^{-26}\,\mathrm{cm^3 s^{-1}}$ is shown for comparison. Central panel: constraints on the parameter space of WIMP annihilating models in the MIN (solid) and MAX (dashed) propagation schemes (see text and Ref. [3] for details). Final states of annihilations are $b\bar{b}$ (blue) and $\mu^+\mu^-$ (orange). Right panel: same as in the central panel, but for decaying DM. Figures adapted from Ref. [3].

spectrum is undermined by uncertainties in the Galactic anisotropies). The decaying model is again less/more favorable for faint/bright fluxes, when compared to the annihilating case. Notice also that it has relatively more power on large scales, as a consequence of the ρ^2 dependence of the signal in the annihilating situation, that enhances the relevance of small scales. Similar considerations apply also to the angular correlation function plotted in the right panel of Fig. 5, with slightly more favorable conclusion for WIMPs.

A caveat is in order here: we have treated the source population given by DM–induced signals as a separate population from AGN and SFG. Actually, any astrophysical source is embedded in a (typically much fainter) DM halo. This means that if one subtracts bright sources to isolate, for instance, sub–μJy sources, she/he might be subtracting also emissions from the corresponding DM halos, and potentially a significant fraction of the total DM contribution can be subtracted as well. Plots in Figs. 4 and 5 are theoretically ideal predictions: experimentally, it could be difficult to fully test the predictions, since observations will be probably biased towards DM sources hosting a faint baryonic counterpart. A possible way to circumvent this problem is to compute the total emission for each structure in the Universe (namely to add together both the DM and astrophysical emissions coming from the same source), and then comparing the results between the cases with/without DM, and applying different brightness cuts. This would require to associate to any DM halo of mass M and redshift z all the different possible astrophysical source populations and spatial distributions in a statistical way. This is theoretically very challenging and deserves a dedicated analysis.

Finally we move to discuss the constraints that can be currently derived on the WIMP DM properties. We conservatively choose not to add any other astrophysical contribution to the theoretical flux, and to compare directly the theoretical predictions for the DM radio emission to the experimental data (summarized in Ref. [3]). Considering the benchmark scenario discussed above, we show in the left panel of in Fig. 6 the bounds arising from total intensity, source counts, and angular correlation. The exclusion curves scales roughly as $M_{\rm DM}^2$ for $M_{\rm DM}$ above few tens of GeV,

while for lighter WIMPs the induced spectra can become significantly softer than data, which leads to a flattening of the curves. Note that the total–intensity bound is subdominant. However, as already mentioned, we have been exploiting extragalactic estimates from the ARCADE collaboration which are 5–6 times larger than the expected emission. Whether this excess will be ascribed to instrumental or galactic contaminations rather than to extragalactic sources, the bound should be accordingly rescaled. Moreover, for different scenarios with an enhanced total emission due to the inclusion of low brightness objects (e.g. reducing $M_{\rm cut}$ or introducing (resolved) substructures), the intensity constraint becomes more effective than number counts since for the latter there are no data at low brightness.

As stressed in Ref. [3], the experimental data currently available make constraints from anisotropies and number counts significantly weaker with respect to what one could in principle achieve with deeper future survey (while the total–intensity bound is not expected to dramatically improve). On the other hand, since DM halos can host much brighter baryonic components, the induced emission of the former can be observationally hidden by the latter for what concerns measurements of number counts and two–point angular correlation function. Here, to derive conservative constraints we consider only total intensity and angular power spectra C_ℓ derived from observations with single–dish telescopes and CMB satellites (which get contributions from sources at all brightnesses). The lowest multipole considered at low (high) frequency is $\ell = 50$ ($\ell = 3000$) because of contaminations from galactic (CMB) anisotropies which make any estimates of extragalactic source contribution on larger scales too uncertain [25, 24, 29].

For our final constraints on WIMP parameter space, we define two sample cases bracketing the effect of quantities which affect the extragalactic DM radio flux but *not* directly related to DM microscopic properties (namely: clustering, substructures, magnetic field, and spatial diffusion). The first scenario (called MIN) is such that the flux is minimized, while the second (MAX) corresponds to the most optimistic assumptions (for a detailed explanation of the choice of parameters for the two configurations, see Ref. [3]). Again two benchmark final states of annihilations (decays), are chosen: $b\bar{b}$ (inducing a softer e^+e^- spectrum) and $\mu^+\mu^-$ (inducing a harder e^+e^- spectrum). The annihilating case is shown in the central panel of Fig. 6, while the decaying case is plotted in the right panel. Although the impact of various single assumptions is quite different in annihilating models with respect to decaying scenarios, there are roughly three orders of magnitude between the MIN and MAX constraints in both cases. Only for low mass WIMPs and fairly optimistic assumptions we can reach the benchmark "thermal" annihilation rate $\langle\sigma_a v\rangle = 3 \cdot 10^{-26}\,{\rm cm}^3{\rm s}^{-1}$. In the decaying case, the inclusion of angular power spectrum data leads to significant improvements with respect to constraints derived from total intensity, especially for large masses (while in the annihilating case the improvement is negligible).

4. The ARCADE excess

Recently, the balloon–borne experiment ARCADE 2 (Absolute Radiometer for Cosmology, Astrophysics and Diffuse Emission) [30] reported radio detection of the sky temperature in the frequency range from 3 to 90 GHz. After subtraction of the foreground galactic emission, an isotropic component has been isolated from the ARCADE data [31]. Surprisingly, the level of this remaining flux (interpreted as an extra–galactic sky temperature) is about 5–6 times larger than the

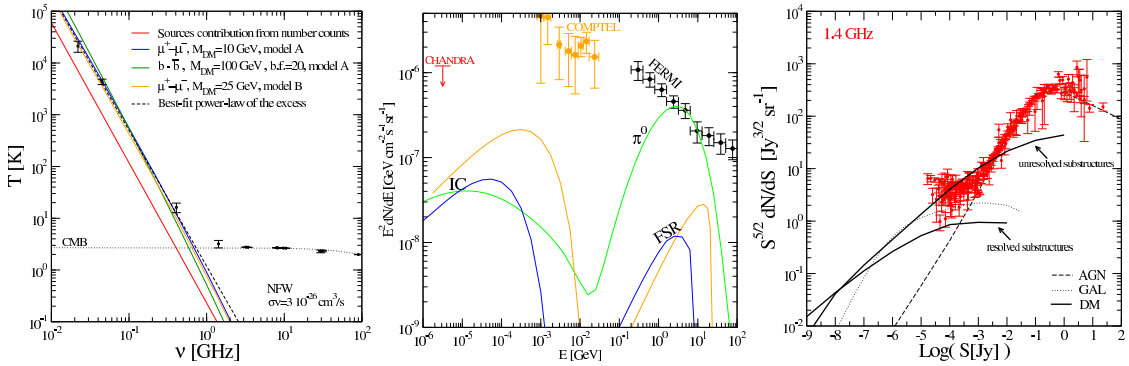

Figure 7: Left panel: Extragalactic radio background as derived by ARCADE [31], together with three possible interpretations of the low–frequency (< 10 GHz) excess in terms of WIMP annihilations (blue, green, and orange curves). The astrophysical source contribution estimated from number counts (red line), the CMB contribution (black–dotted line), and a best–fit power–law of the excess (black–dashed line) are also shown [19]. Central panel: X–ray and gamma–ray fluxes for the three benchmark WIMP cases shown in the left panel, together with the CHANDRA [32] bound in the X–ray band, and the COMPTEL [33] and FERMI [34] extragalactic gamma–ray flux measurements. Right panel: differential number counts of active galactic nuclei (dashed line), star–forming galaxies (dotted line), and the same 10 GeV benchmark DM model (solid lines) shown in the left panel. For DM, we consider two cases: all substructures are resolved; all substructures are unresolved. For data and astrophysical models, see [20] and references therein. Figures adapted from Ref. [1].

total contribution from the extra–galactic radio sources detected in current surveys [19, 35]. Even extrapolating the source number counts to lower (currently unreached) brightness, such excess persists. Most systematic effects which could explain the ARCADE excess have been ruled out [31] and an astrophysical galactic origin appears to be quite unlikely [36, 37]) Free–free emission has been excluded on the basis of the spectral shape, and a diffuse Galactic synchrotron foreground is estimated using two different methods (a simple co–secant dependence on the Galactic latitude and a correlation between radio and atomic line emissions), which agree well among each other.

Such level of cosmic radio background does not have an immediate explanation in standard astrophysical scenarios. In Ref. [37], radio supernovae, radio quiet quasars and diffuse emission from intergalactic medium and clusters (together with a missed flux from well–known sources) have been considered: Ref. [37] concludes that none of these emissions can significantly contribute. A new, currently unknown, population of abundant and faint radio sources (able to dominate source–counts around μJy fluxes) needs to be introduced [37, 38]. A possibile solution could be offered by rdinary star–forming galaxies with a radio to far–infrared flux ratio which increases significantly with redshift. However, this possibility is strongly constrained by multi–wavelength observations. Indeed, the radio to far–infrared emission would need to be increased by a factor of five above what is currently observed in local galaxies. An explanation of the ARCADE excess through radiative emission of secondary electrons in SFG would actually overproduce the gamma–ray background from pion decays [39]. The same occurs also for primary electrons, unless such galaxies possess either extremely low gas density (and, consequently, low ratio of primary electrons to pions) or extremely efficient proton escape. The picture that is currently emerging from the ARCADE measurements [31, 37] and subsequent interpretations [37, 38, 39, 40] suggests the need

for a population of several faint synchrotron–sources prompted by primary electrons with a hard spectrum and with no or very faint correlated mechanisms at infrared and gamma–ray frequencies.

Synchrotron emission due to electron/positrons produced by DM annihilation or decay in the extragalactic environment can offer a solution to this significant radio excess [1]. Considering the current understanding of structure clustering, any luminous source is embedded in a DM halo, and therefore extragalactic DM halos can be seen as the most numerous source population. The radio flux induced by WIMP annihilations or decays is predicted to be very faint. WIMP models with large annihilation or decay into leptons induce hard spectra of e^+/e^- with very faint gamma–ray counterpart (and no straightforward thermal emission). Therefore, WIMP emission represent an ideal candidate to fit the ARCADE excess [1].

The radio excess spectrum reported by ARCADE is rather hard, and this requires a hard electron/positron spectrum. Such a behavior can be obtained in DM scenarios where WIMPs annihilate or decay mostly into leptons. In the left panel of Fig. 7 we show the case of annihilation in the $\mu^+\mu^-$ channel. The absolute normalization of the excess is reproduced with a "thermal" annihilation rate $\langle\sigma_a v\rangle = 3 \cdot 10^{-26}\mathrm{cm}^3\mathrm{s}^{-1}$ and a DM mass around 10 GeV: even though this candidate induces a spectrum slightly softer than the best–fit power–law, it provides a reasonable agreement with the data. The fact that light DM, in the 10 GeV mass range, can fairly well reproduce the ARCADE excess, without the need of unrealistically large DM overdensities is particularly interesting, especially in light of recent indications coming from direct detection experiments (DAMA [16], CoGeNT [17], and CRESST [18]), that can be in fact accommodated with a ~ 10 GeV WIMP.

Since the ARCADE excess could be due to by DM annihilation/decay into electrons and positrons, production of X–rays and gamma–rays by means of inverse–Compton processes on interstellar radiation fields and direct production of gamma–rays from the DM particle annihilation (either by production of neutral pions or by Final–State–Radiation (FSR)) are present. For the benchmark cases considered here, these multi–wavelength bounds are easily evaded, as shown for X- and γ-rays in the central panel of Ref. 7.

As a further analysis on the radio emission arising from light DM annihilation/decay, able to explain to the ARCADE excess, we show in Fig. 7 the differential number counts of sources at the frequency of 1.4 GHz. When all substructures are assumed to be unresolved, they mainly boost the signal of large and bright halos (since the latter host more sub–halos). On the contrary, if it is possible to resolve all substructures, number counts drop much more slowly at low brightness. To bracket the uncertainties related to the possibility of resolving or not substructures, the two extreme cases are shown in Fig. 7 as solid lines, for the same 10 GeV DM particle shown in the left panel. As discussed above, the key point for our analysis is that in both scenarios the number of DM sources undoubtly becomes dominant over the astrophysical contributions (AGN, SFG) at the sub-μJy level. The contribution of SFG, dominant over AGN emission at low fluxes, decreases more rapidly than the expected contribution from DM (assuming FIR/radio correlation holds at all redshift), both for resolved and unresolved substructures. From 7 we notice that the flattening at low brightness exhibited by current data, although it can be easily accounted for by standard astrophysical populations, nevertheless could be well fitted by a DM model between the two extreme cases presented in Fig. 7.

Therefore the possibility that synchrotron emission induced by WIMP annihilations can account for the isotropic radio component measured by the ARCADE 2 Collaboration appears to be

a viable possibility. A population of sources which can explain ARCADE measurements has to become the most abundant at brightness around and below the μJy level: this will be studied in details by SKA [41], and hopefully also by its precursors, ASKAP [42] and MeerKAT [43]. A dedicated study of closest and brightest (in terms of DM–induced signal) objects with current radio telescope (e.g., ATCA [44] and EVLA [45]) can start to probe this scenario in the near future.

5. Conclusions

In this note we have discussed the relevance of radio signals for WIMP dark matter detection. We have seen that radio emission in the MHz–GHz frequency range may be easily produced by DM annihilation/decay in our Galaxy or in the extragalactic environment and that this radio emission may be at the level of detectability with current or foreseen radio detectors.

Under reasonable assumptions on the DM distribution and on the astrophysical magnetic fields, radio signals are already able to pose bounds on WIMP dark matter comparable to other indirect detection searches: in fact, the galactic radio emission is close to detectability for "thermal" annihilation cross sections for light DM and NFW halo profiles. In particular, low–frequency surveys are quite competitive to search for light DM particles. Potential channels of discovery are offered by source number counts at low brightnesses (below the μJy level) and angular correlations of the radio sky temperature at low multipoles and low brightnesses. In order to be able to properly access these channels, increased sensitivities are necessary, but the foreseen experiments appear to be well suited to approach them.

The prediction of the radio emission requires the knowledge of a large number of astrophysical inputs: not only the dark matter distribution in galaxies and in the extragalactic systems, but also the modeling of electron/positron transport phenomena (propagation and energy losses), as well the size and distribution of galactic and extragalactic magnetic fields. Among the DM indirect detection signals, the radio signal is maybe the one most affected by sources of uncertainty: nevertheless, it possesses specific features which make it unique and, considering the promising future that foresees the development of many new, high–sensitivity detectors (like ASKAP, MeerKAT, LOFAR, SKA), the radio channel for DM detection may well produce interesting surprises. Stay tuned!

We thank the Center for Theoretical Underground Physics and Related Areas (CETUP* 2012) in South Dakota (USA) for its hospitality and for partial support during the completion of this work. We acknowledge research grants funded jointly by Ministero dell'Istruzione, dell'Università e della Ricerca (MIUR), by Università di Torino and by Istituto Nazionale di Fisica Nucleare within the *Astroparticle Physics Project* (MIUR contract number: PRIN 2008NR3EBK; INFN grant code: FA51). We also acknowledge the spanish MICINN Consolider Ingenio 2010 Programme under grant MULTIDARK CSD2009- 00064 for support.

References

[1] N. Fornengo, R. Lineros, M. Regis and M. Taoso, *Phys. Rev. Lett.* **107**, 271302 (2011) [arXiv:1108.0569 [hep-ph]].

[2] N. Fornengo, R. A. Lineros, M. Regis and M. Taoso, *JCAP* **1201**, 005 (2012) [arXiv:1110.4337 [astro-ph.GA]].

[3] N. Fornengo, R. Lineros, M. Regis and M. Taoso, *JCAP* **1203**, 033 (2012) [arXiv:1112.4517 [astro-ph.CO]].

[4] E. Borriello, A. Cuoco and G. Miele, *Phys. Rev. D* **79** (2009) 023518 [arXiv:0809.2990 [astro-ph]].

[5] C. Boehm, T. Delahaye and J. Silk, *Phys. Rev. Lett.* **105** (2010) 221301 [arXiv:1003.1225 [astro-ph.GA]].

[6] G. Bertone, G. Sigl and J. Silk, *Mon. Not. Roy. Astron. Soc.* **337** (2002) 98 [astro-ph/0203488].

[7] C. Boehm, J. Silk and T. Ensslin, arXiv:1008.5175 [astro-ph.GA].

[8] R. M. Crocker, N. F. Bell, C. Balazs and D. I. Jones, *Phys. Rev. D* **81** (2010) 063516 [arXiv:1002.0229 [hep-ph]].

[9] M. Regis and P. Ullio, *Phys. Rev. D* **78** (2008) 043505 [arXiv:0802.0234 [hep-ph]].

[10] L. Bergstrom, G. Bertone, T. Bringmann, J. Edsjo and M. Taoso, *Phys. Rev. D* **79** (2009) 081303 [arXiv:0812.3895 [astro-ph]].

[11] G. Bertone, M. Cirelli, A. Strumia and M. Taoso, *JCAP* **0903** (2009) 009 [arXiv:0811.3744 [astro-ph]].

[12] D. T. Cumberbatch, J. Zuntz, H. K. K. Eriksen and J. Silk, arXiv:0902.0039 [astro-ph.GA].

[13] G. Dobler and D. P. Finkbeiner, *Astrophys. J.* **680** (2008) 1222 [arXiv:0712.1038 [astro-ph]].

[14] T. Linden, S. Profumo and B. Anderson, *Phys. Rev. D* **82** (2010) 063529 [arXiv:1004.3998 [astro-ph.GA]].

[15] D. Hooper, D. P. Finkbeiner and G. Dobler, *Phys. Rev. D* **76** (2007) 083012 [arXiv:0705.3655 [astro-ph]].

[16] R. Bernabei *et al.*, *Eur. Phys. J.* C 56 (2008) 333; *Eur. Phys. J.* C **67**, 39 (2010).

[17] C.E. Aalseth *et al.*, arXiv:1106.0650 [astro-ph.CO].

[18] G. Angloher *et al.*, [arXiv:1109.0702 [astro-ph.CO]].

[19] M. Seiffert *et al.*, arXiv:0901.0559 [astro-ph.CO].

[20] G. De Zotti *et al.*, Astron. Astrophys. Rev. **18** (2010)

[21] S. Profumo, T. E. Jeltema, *JCAP* **0907** (2009) 020. [arXiv:0906.0001 [astro-ph.CO]].

[22] C. Blake, P. G. Ferreira, J. Borrill, emphMon. Not. Roy. Astron. Soc. **351** (2004) 923. [astro-ph/0404085].

[23] Haslam, C. G. T., Salter, C. J., Stoffel, H., & Wilson, W. E., *A&AS*, **47** (1982) 1.

[24] M. Regis, [arXiv:1101.5524 [astro-ph.HE]].

[25] L. La Porta *et al.*, *Astron. Astrophys.* **479** (2008) 641 [arXiv:0801.0547].

[26] C. L. Reichardt *et al.*, [arXiv:1111.0932 [astro-ph.CO]].

[27] O. Adriani *et al.* [PAMELA Collaboration], *Nature* **458** (2009) 607 [arXiv:0810.4995 [astro-ph]].

[28] R. A. Overzier, H. J. A. Rottgering, R. B. Rengelink, R. J. Wilman, *Astron. Astrophys.* **405** (2003) 53-72. [astro-ph/0304160].

[29] G. Giardino, *et al.*, *Astron. Astrophys.* **371** (2001) 708 [astro-ph/0103233]. *Astron. Astrophys.* **387** (2002) [astro-ph/0202520].

[30] J. Singal *et al.*, *Astrophys. J.* **730** (2011) 138.

[31] D. J. Fixsen *et al.*, arXiv:0901.0555 [astro-ph.CO].

[32] R. C. Hickox and M. Markevitch, *Astrophys. J.* **661** (2007) L117.

[33] G. Weidenspointner *et al.* in *American Institute of Physics Conference Series* **510** (2000) 467-470.

[34] A. A. Abdo *et al.* [The Fermi-LAT Collaboration], *Phys. Rev. Lett.* **104** (2010) 101101.

[35] M. Gervasi *et al.*, *Astrophys. J.* **682** (2008) 223.

[36] A. Kogut *et al.*, *Astrophys. J.* **734** (2011) 4.

[37] J. Singal *et al.*, *MNRAS* **409** (2010) 1172.

[38] T. Vernstrom *et al.*, arXiv:1102.0814 [astro-ph.CO].

[39] B. C. Lacki, *Astrophys. J.* **729** (2011) L1.

[40] P. P. Ponente *et al.*, arXiv:1104.3012 [astro-ph.CO].

[41] S. Rawlings, R. Schilizzi, arXiv:1105.5953 [astro-ph.IM]. http://www.skatelescope.org/

[42] S. Johnston *et al.* [ASKAP Collaboration], *PoS* **MRU** (2007) 006. [arXiv:0711.2103 [astro-ph]];

[43] R. S. Booth *et al.*, arXiv:0910.2935 [astro-ph.IM]; http://www.ska.ac.za/meerkat/

[44] http://www.narrabri.atnf.csiro.au/

[45] https://science.nrao.edu/facilities/evla